Novel synthesis of Cl/N Co-doped TiO_2 nanoparticles for enhanced photocatalytic activity

S. Wannapop*, A. Inteng, R. Jareanwat, A. Somdee
Faculty of Science, Energy and Environment, King Mongkut's University of Technology North Bangkok, Rayong Campus, Rayong 21120, Thailand

The N/Cl co-doped TiO_2 nanostructures were studied as photocatalyst for rhodamine B (RhB), Methylene Blue (MB), and Methyl Orange (MO) degradation. A Commercial TiO_2 (P25) grade was also compared to our materials. The N/Cl co-doped TiO_2 at different Ti^{4+} precursors were synthesized by the co-precipitation method. The structural, surface morphology, and surface area were analyzed by XRD, SEM, TEM, and BET. Optical properties of samples were investigated by UV-visible spectroscopy showing that the N/Cl co-doped TiO_2 has smaller bandgap than the P25. Overall, the improved N/Cl co-doped TiO_2 samples showed better performance than the P25 for RhB, MB and MO degradations.

(Received March 31, 2024; Accepted July 1, 2024)

Keywords: Photocatalyst, Nanocomposites, SEM, TEM,XRD

1. Introduction

Titanium dioxide (TiO_2) is currently preferred as the most widely used and effective photocatalyst for decomposing organic pollutants in water. The TiO_2 is a low-cost semiconductor. It is non-toxic to the environment, with strong oxidizing properties and long-term light stability [1-4]. However, titanium dioxide's ability to absorb sunlight has its limitations. Due to the large band gap (3.2 eV), TiO_2 functions properly in the ultraviolet (UV) light range. Solar energy contains only 5% of sunlight's ultraviolet radiation. Therefore, most of the energy from solar radiation that could have been used to promote TiO_2-catalyzed reactions is wasted. The solar absorption capacity of TiO_2 has been developed by various methods such as doping with a metal, non-metal, metal oxide, and co-doping [5-8]. In addition, the enhancement of photocatalytic activity of TiO_2 is significantly affected by crystal size, surface area, porosity, crystal structure, and crystallinity.

Recent researchers have been interested in chemical and physical doping to increase the photocatalytic activity of TiO_2 under visible light irradiation, such as TiO_2 doping with metals (*e.g.* Mn, Fe, Cu, Ag, Au, and Pt [9-13]) or non-metals (S, N, C, and Cl [14, 15]) can absorb the visible light (400–700 nm). Doping metal/non-metal atoms into TiO_2 also increases conductivity. Comparing the metal and chalcogenide or nitrogen group, the cost of using metal is much more expensive. From a theoretical point of view, the role of doping metal is to modify the conduction energy band edge of TiO_2 materials. Since the metal is mostly substituted into the Ti of TiO_2 host material. In contrast to the halogenide or nitrogen group, the valence band edge of TiO_2 was modified instead. In particular, the addition of nitrogen or chloride is considered a very efficient way to extend the UV absorbance to the visible region because the band gap is narrowed by the N_{2p} state with the O 2p [16,17], as in the similar case of chlorine with a mixture of Cl 2p and O 2p states [18]. The Cl and N doped TiO_2 individually had been studied in many previous works. Interestingly, the structural surface morphology of the products was different depending on the various synthesis methodologies, such as the pH control [19, 20], the total amount of doping materials, and the heating treatments [21-23]. In particular, none of the research studied the role of N/Cl co-doping in the TiO_2.

This study demonstrates that a co-precipitation method can be prepared for a Cl/N-doped TiO_2 nanoparticle photocatalyst with improved visible light absorption. It also studied the influence of the Ti precursor on the characteristics of the synthesis structure, morphology, and optical properties.

* Corresponding author: surangkana.w@sciee.kmutnb.ac.th
https://doi.org/10.15251/DJNB.2024.193.999

The product's crystal structure was characterized by X-ray diffraction. Surface properties were studied using scanning electron microscopy, transmitted electron microscopy, and Brunauer-Emmett-Teller. The optical properties of all photocatalysts were studied by UV-visible absorption. The catalyst products of the commercial TiO_2 P25 grade and our Cl/N co-doped TiO_2 were compared for photocatalytic activity by Rhodamine B (RhB) under solar simulator radiation.

Then, the best catalytic was tested with another dye, such as Methylene Blue (MB) and Methyl Orange (MO).

2. Experimental

The N/Cl co-doped TiO_2 was synthesized by co-precipitation using different precursors of Ti, which were titanium (IV) isopropoxide ($C_{12}H_{28}O_4$ Ti), titanium (IV) tetrachloride ($TiCl_4$), and titanium (IV) butoxide ($TiC_{16}H_{36}O_4$). First, 2 mL of each Ti source was dissolved in a mixing solution (80 ml of deionized water and 20 ml of HCl, which acted as a chlorine source) under vigorous stirring. Then, the solution was controlled at pH = 11 by ammonia, a nitrogen source, and vigorously stirred for 2 h. The final products were washed with DI water and ethanol, and the samples were dried at 100 °C for 5 h. The products were annealed at 500 °C in nitrogen air for 2 h. For the purpose of comparison, the N/Cl co-doped TiO_2 using $C_{12}H_{28}O_4$ Ti as the source was denoted as "NCl-TiO_2-1". The product from the $TiCl_4$ source is identified as "NCl-TiO_2-2," and the one from the $TiC_{16}H_{36}O_4$ source was designated as "NCl-TiO_2-3". Commercial P25 was denoted as "P25-TiO_2". The products were characterized by XRD (Bruker AXS D8 eco), TEM (JEOL JEM-2010), SEM (JEOL, JSM 6335F), and BET (Quantachrome Instruments, Autosorb-iQ-MP-MP).

The samples were tested for photocatalytic activity of dye photodegradation (RhB, MB, and MO) under a xenon lamp with a similar light intensity. A sample of 0.2 g was dispersed in 200 ml of RhB, MB, and MO aqueous solution at a concentration of $1x10^{-5}$ M. A solution was kept in the dark and stirred for 30 min to active dye absorption-desorption equilibrium. A 5 ml sample of each solution was collected and centrifuged every 10 min for photocatalytic testing. The residual RhB, MB, and MO concentrations were measured by UV-visible spectrophotometry (Shimadzu UV-2600) at the peak wavelengths of 553 nm, 663 nm, and 464 nm, respectively.

3. Results and discussions

The XRD patterns of Pure TiO_2 (P25) and N/Cl co-doped TiO_2 with different precursors are shown in Fig.1. For the N/Cl co-doped TiO_2 sample, there was one phase originating from the TiO_2: anatase (JCPDS no. 21-1272) [24]. The diffraction peak position of 2θ located at 25.16°, 36.88°, 37.71°, 38.55°, 47.98°, 53.83°, 55.10°, 62.64°, and 68.73° corresponds to (101), (103), (004), (112), (200), (105), (211), (204), and (116) plane, respectively. The results showed that the diffraction pattern of P25-TiO_2 matched two phases: anatase (JCPDS no. 21-1272) and rutile (JCPDS no. 21-1276). In case of anatase, the diffraction peaks of P25 located at 25.22°, 25.88°, 37.71°, 38.50°, 47.92°, 53.83°, 55.01°, and 62.58° which corresponds to the plane (101), (103), (004), (112), (200), (105), (211), (204), and (116), respectively. TiO_2 rutile, the diffraction peak at 27.23°, 35.93°, 41.17°, and 56.51° is assigned to the (100), (101), (111), and (220) plane.

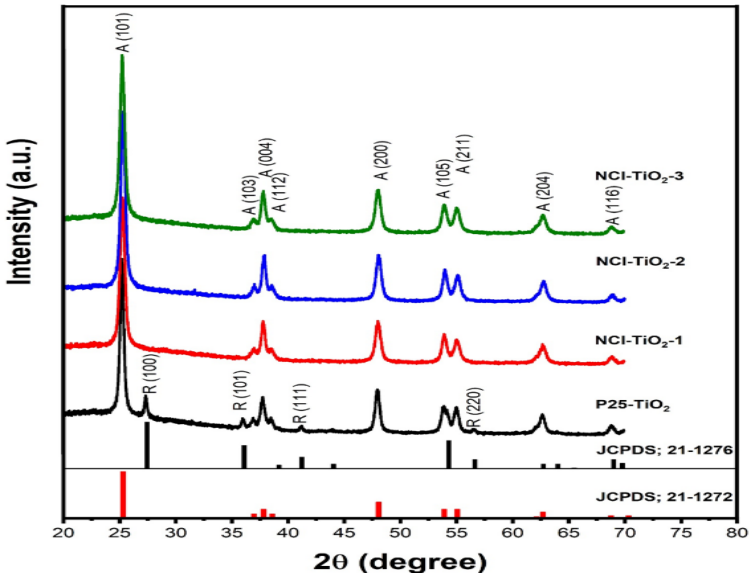

Fig. 1. XRD patterns of P25-TiO_2, NCl-TiO_2-1, NCl-TiO_2-2, and NCl-TiO_2-3, respectively.

Fig. 2 shows SEM image of the P25-TiO_2 and N/Cl co-doped TiO_2. From the top view of the commercial P25 and the modified TiO_2 SEM images, the shapes of commercial P25 and N/Cl co-doped TiO2 are nanoparticles, and the shapes were similar. It will be found that the surface of N/Cl co-doped TiO_2 is slightly rougher than that of commercial P25.

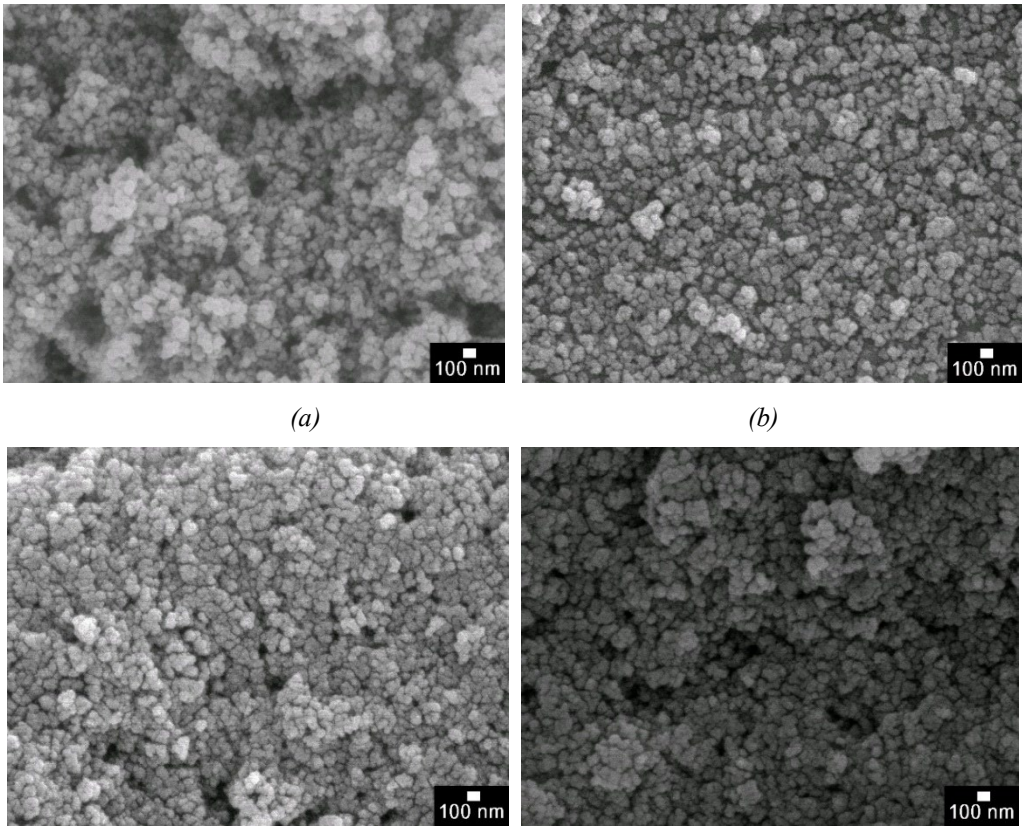

(a) *(b)*

(c) *(d)*

Fig. 2. SEM images of (a) P25-TiO_2, (b) NCl-TiO_2-1, (c) NCl-TiO_2-2, (d) NCl-TiO_2-3.

In Fig. 3, the EDS mapping and EDS spectrum investigation revealed the N and Cl contained in the NCl-TiO_2-3 sample. The EDS analysis was used to report the interest element of the target sample. Therefore, the N, Cl, Ti, and O were of interest to us. From the result, the EDS confirmed all elements, as mentioned before, were observed, which suggests that the N and Cl co-doping was successfully obtained.

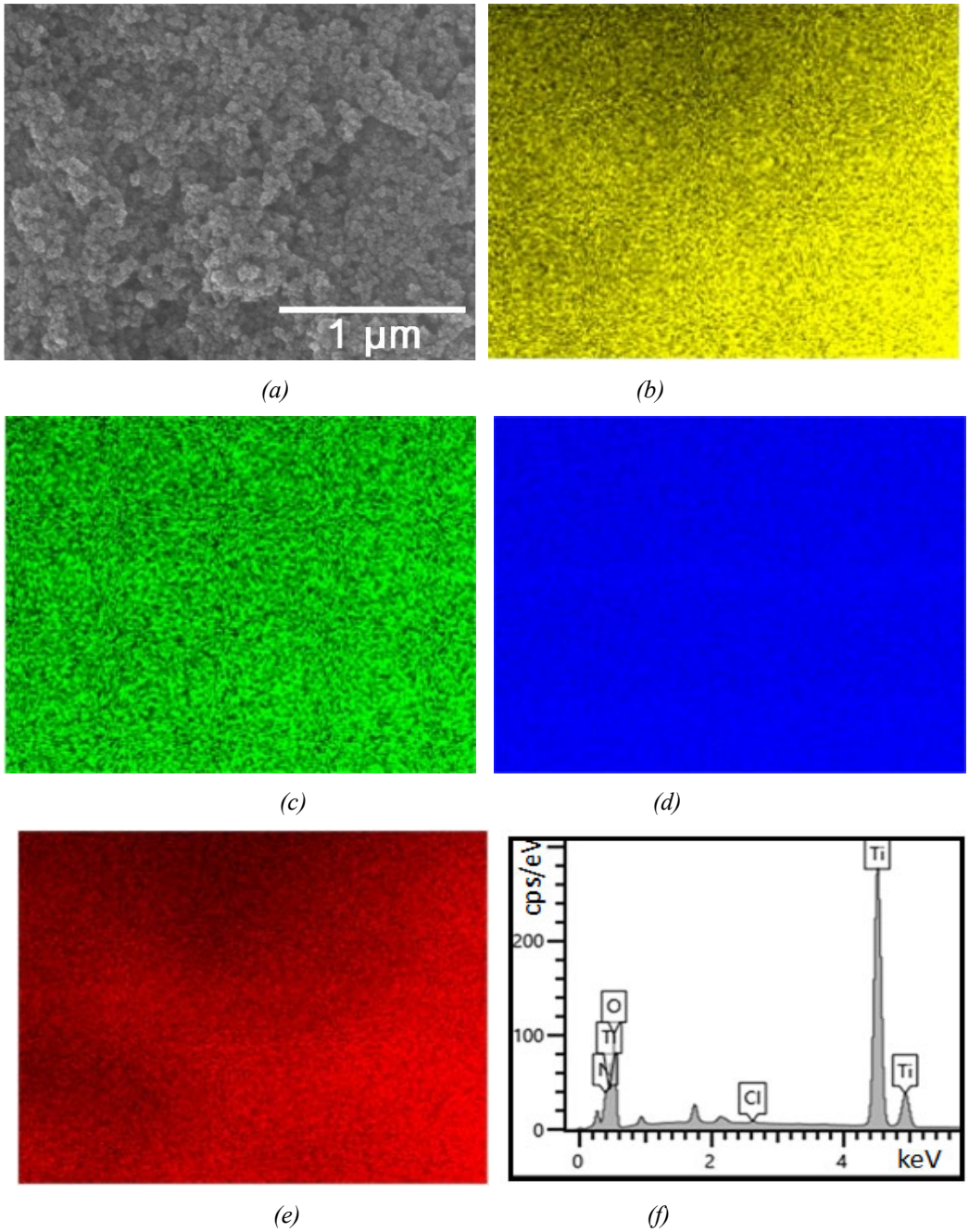

Fig. 3. (a) SEM image and EDS mapping of (b) N, (c) Cl, (d) Ti, (e) O, and (f) EDX spectrum of NCl-TiO_2-3.

Fig. 4 shows the TEM image, HRTEM image, and Particle diameters from TEM images. In Fig. 4b, the HRTEM image of P25-TiO_2 indicates that the lattice fringes correspond to (211) and (105) plans from anatase TiO_2 and rutile TiO_2, respectively. The NCl-TiO_2-1 HRTEM is shown in Fig. 4e. The lattice fringes correspond to (105) plans from anatase TiO_2. In Fig. 4h and Fig. 4k, the lattice fringes correspond to (004) planes from anatase, TiO_2 from NCl-TiO_2-2, and NCl-TiO_2-3,

respectively. From the HRTEM image, N/Cl co-doped TiO_2 had one phase of anatase TiO_2, consistent with the XRD results and that of P25-TiO_2 with two phases. From the TEM image, the surface of N/Cl co-doped TiO_2 has a greater roughness than pure TiO_2, consistent with SEM results. The average particle sizes of commercial P25 and N/Cl co-doped TiO_2 are shown in Fig. 4(c, f, i, and l). The average size of P25-TiO_2, NCl-TiO_2-1, NCl-TiO_2-2, and NCl-TiO_2-3 samples are about 19.10, 20.35, 21.43, and 19.95 nm, respectively. Fig. 5 shows the BET surface areas of the modified TiO_2 nanoparticles were 68.71, 65.02, and 69.90 m^2/g for NCl-TiO_2-1, NCl-TiO_2-2, and NCl-TiO_2-3, respectively, and BET surface area of commercial P25 was 52.36 m^2/g. These values are in good agreement with Fig. 4, which estimated the particle size of the sample by TEM.

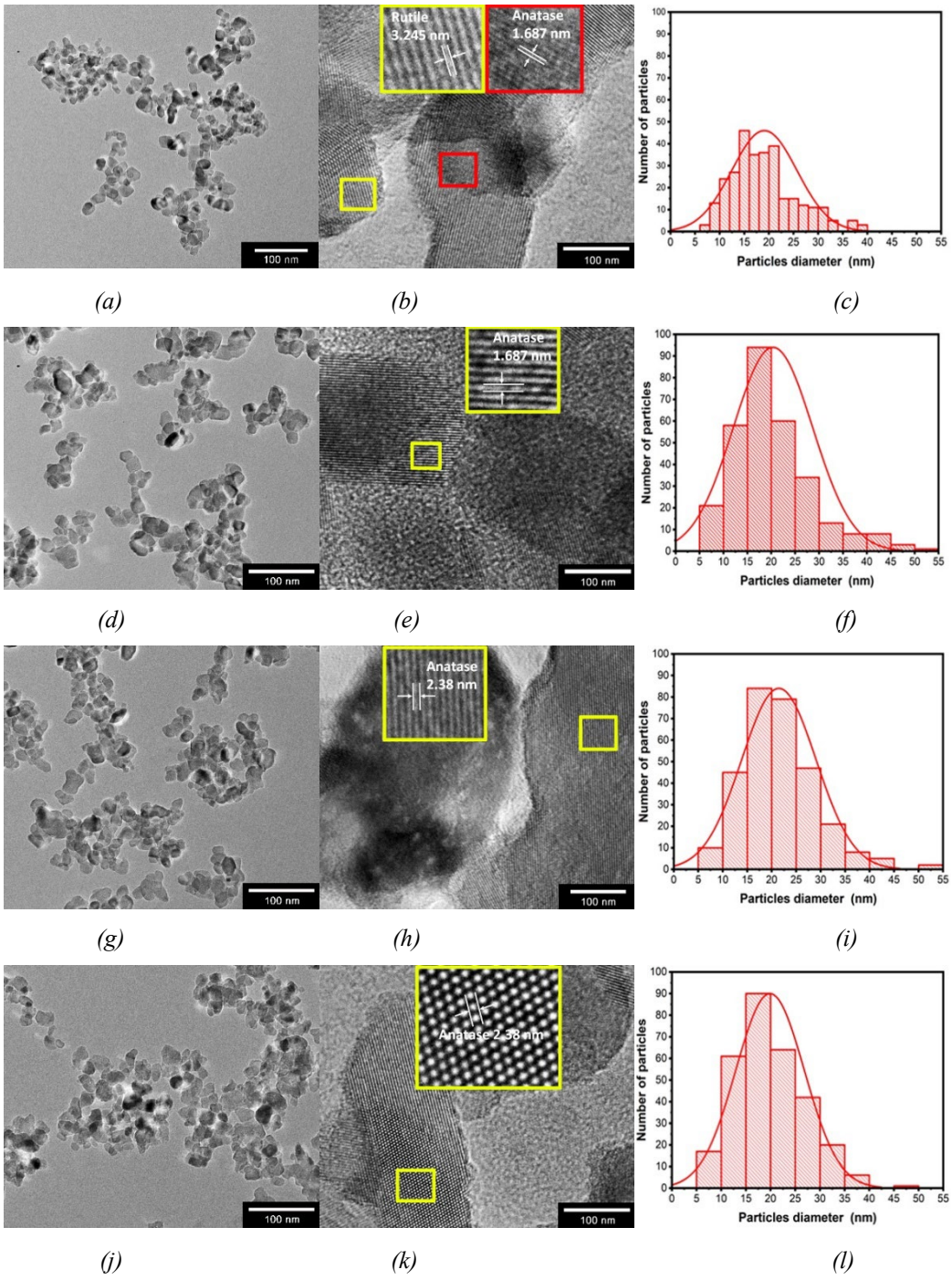

Fig. 4. TEM images, HRTEM images, and particle diameters of (a-b) P25-TiO_2, (c-d) NCl-TiO_2-1, (e-f) NCl-TiO_2-2, and (g-h) NCl-TiO_2-3, respectively.

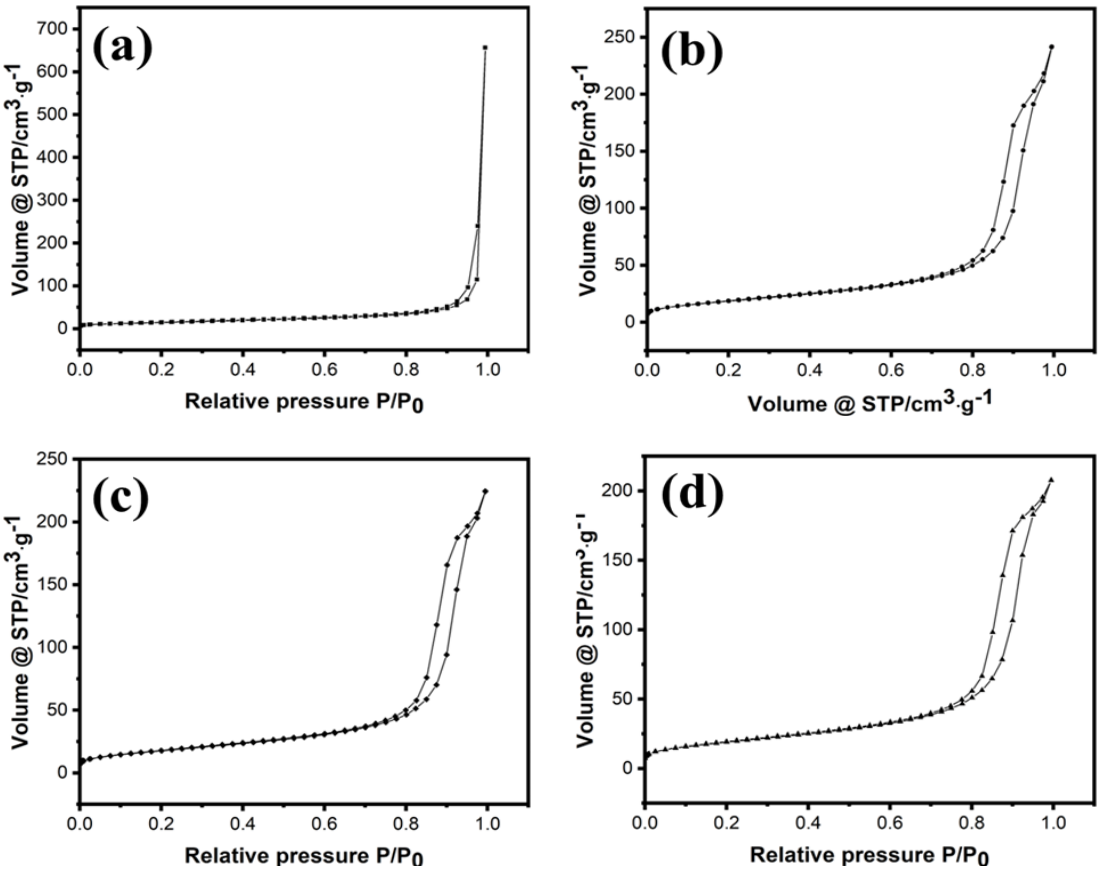

Fig. 5. BET surface area measurements of (a) P25-TiO_2, (b) NCl- TiO_2-1, (c) NCl- TiO_2-2, and (d) NCl-TiO_2-3, respectively.

Fig. 6a shows the optical properties of TiO_2-P25 and the N/Cl co-doped TiO_2 products as determined by UV-visible spectroscopy. The energy band edge of P25 was located at ~400 nm while the N/Cl co-doped TiO_2 was slightly located at the lower energy. These results of doping were in agreement with similar previous work [25, 26]. In this research, the N/Cl co-doped TiO_2 products showed better absorption than commercial P25. Photocatalytic activities of the commercial P25 and N/Cl co-doped TiO_2 catalysts were evaluated by decomposed RhB molecules under solar light radiation. Fig. 6b and Fig. 6c show the degradation efficiency using RhB solution as the model dye, the blank (catalyst-free), commercial P25, and N/Cl co-doped TiO_2 photocatalysts under solar light radiation within 80 min. There is slight light-induced self-degradation of RhB molecules with the blank. From N/Cl co-doped TiO_2 photocatalysts degradation tested by synthesized by co-precipitation from different Ti sources, it was found that the decolorization increased over time. In 80 min, the NCl-TiO_2-3 shows the highest decolorization efficiency of 99.12%. This is because NCl-TiO_2-3 had a large surface area (see the BET and particle size derived from TEM results) and, therefore, more reactive regions areas on the surface for the adsorption of the dye molecules, making the photocatalytic process more efficient.

Furthermore, the stability of the NCl-TiO_2-3 photocatalyst was also tested. Fig. 7a shows the 3rd recycling used for RhB removal, while Fig. 7b shows other dye treatments. The performance of the NCl-TiO_2-3 photocatalyst was also examined with MB and MO. The degradation efficiency, which reveals the performance of the NCl-TiO_2-3 sample, is shown in Fig. 7b. After up to 80 min solar light illumination, 99.12% of the RhB was removed, while 92.46 % of the MB, and 53.20% of the MO were removed from the water. As a result, NCl-TiO_2-3 is a great photocatalyst that can degrade RhB, MB, and MO.

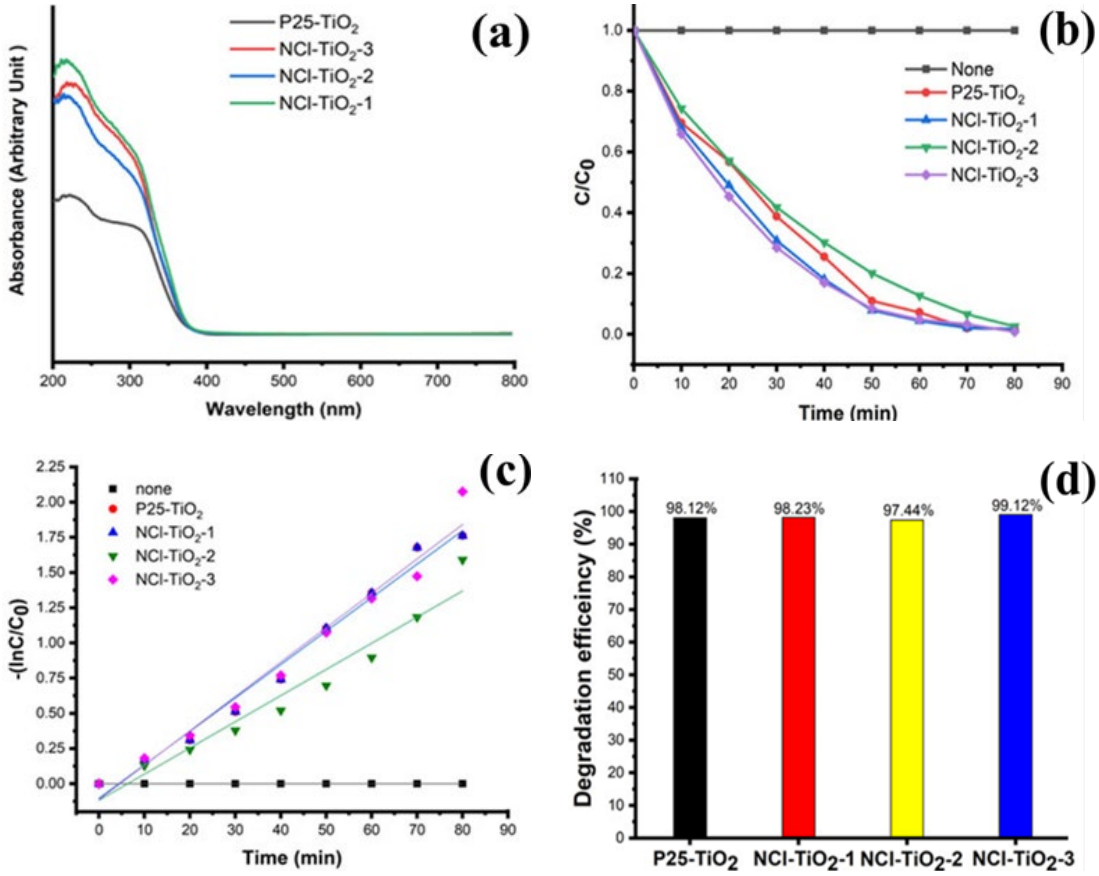

Fig. 6. (a) UV-Vis spectrophotometry, (b) C/Co Vs min, (c) first-order plots for the photocatalytic degradation of RhB over N/Cl co-doped TiO_2 and Commercial P25, and (d) degradation efficiency of NCl-TiO_2 catalysis and Commercial P25 using RhB dyes.

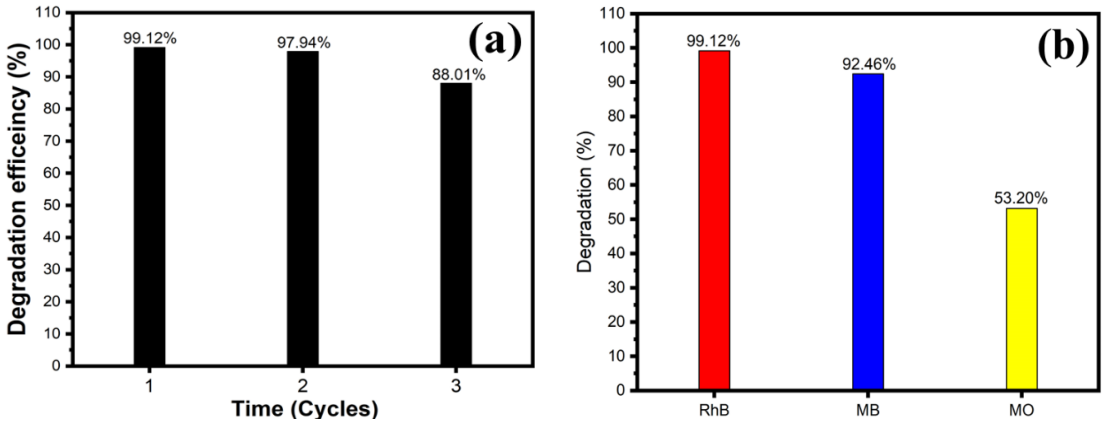

Fig. 7. (a) reuses the third cycle of photocatalytic activity of RhB degradation over NCl-TiO_2-3. (b) the degradation efficiency of NCl-TiO_2 catalysis using RhB, MB, and MO dyes.

In Fig. 8, the structure of the NCl-TiO_2-3 sample was investigated before being applied as the photocatalyst to degradation. After passing the 3rd treatment, the XRD still showed the crystalline of NCl-TiO_2-3 would not be destructive according to the treatment.

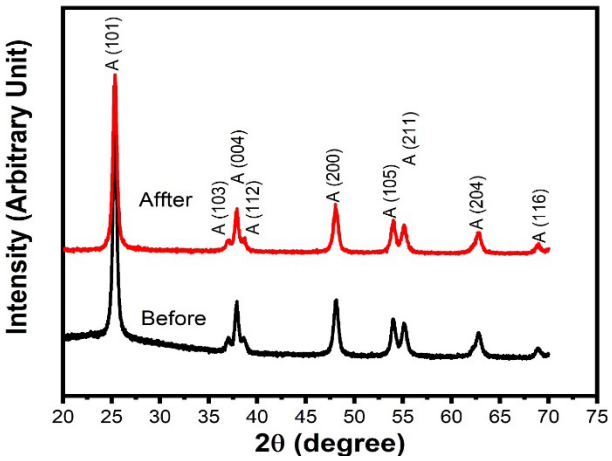

Fig. 8. XRD patterns of NCl-TiO_2-3 before and after reuse Tirth cycles of photocatalytic activity.

4. Conclusions

The N/Cl co-doped TiO_2 nanoparticles were successfully synthesized by the co-precipitation method. The photocatalytic activities via photodegradation were investigated, and the TiO_2 P25 was also studied to compare them with our materials. The NCl-TiO_2-3, using titanium (IV) butoxide ($TiC_{16}H_{36}O_4$) as the Ti source, has the highest dye degradation efficiency of 99.12% within 80 min.

Moreover, the degradation of MB and MO by the NCl-TiO2-3 photocatalyst was studied. This photocatalyst can also degrade over ~53% of the MB and MO dyes. For this reason, NCl-TiO2-3 is recommended as a good photocatalyst for degrading various organic dyes in contaminated wastewater.

Acknowledgments

This research was funded by King Mongkut's University of Technology North Bangkok. Contract no. KMUTNB-64-KNOW-34.

References

[1] X. Zhang, C. Bo, S. Cao, Z. Cheng, Z. Xiao, X. Liu, T. Tan, L. Piao, Journal of Materials Chemistry A (10), 24381-24387, (2022); https://doi.org/10.1039/D2TA06961J
[2] Y. Chen, L. Soler, C. Cazorla, J. Oliveras, N. G. Bastus, V. F. Puntes, J. Llorca, Nature communications 14, 6165, (2023); https://doi.org/10.1038/s41467-023-41976-2
[3] R. A. Carcel, L. Andronic, A. Duta, Materials Characterization 70, 68-73, (2012); https://doi.org/10.1016/j.matchar.2012.04.021
[4] T. Watanabe, S. takawane, Y. Baba, J. Akaiwa, A. Kondo, T. Ohba, The journal of Physical Chemistry C 127, 16861-16869, (2023); https://doi.org/10.1021/acs.jpcc.3c03619
[5] D. Wibowo, M. Z. Muzakkar, S. K. Md. Saad, F. Mustapa, M. Maulidiyah, M. Nurdin, A. A. Umar, Journal of Photochemistry and Photobiology A: Chemistry 398, 112589, (2020); https://doi.org/10.1016/j.jphotochem.2020.112589
[6] M. Misra, N. Singh, R. K. Gupta, Catalysis Science & Technology 7, 570-580, (2017); https://doi.org/10.1039/C6CY02085B
[7] S. S. Ghumro, B. Lai, T. Pirzada, ACS Omega 7, 4333-4341, (2022); https://doi.org/10.1021/acsomega.1c06112
[8] A. Mancuso, O. Sacco, D. Sannino, S. Pragliola, V. Vaiano, Arabian Journal of Chemistry 13 (11), 8347-8360, (2020); https://doi.org/10.1016/j.arabjc.2020.05.019

[9] C. Thambiliyagodage, L. Usgodaarachchi, Current Research in Green and Sustainable Chemistry 4, 100186, (2021)' https://doi.org/10.1016/j.crgsc.2021.100186
[10] H. Chakhtouna, H. Benzeid, N. Zari, A. Qaiss, R. Bouhfid, Environmental Science and Pollution Research 28, 44638-44666, (2021); https://doi.org/10.1007/s11356-021-14996-y
[11] Y. Yu, W. Wen, X.-Y. Qian, J.-B. Liu, J.-M. Wu, Scientific reports 7, 41253, (2017); https://doi.org/10.1038/srep41253
[12] T. Ali, A. Ahmed, U. Alam, I. Uddin, P. Tripathi, M. Muneer, Materials Chemistry and Physics 212, 325-335, (2018); https://doi.org/10.1016/j.matchemphys.2018.03.052
[13] N. Sharotri, D. Sharma, D. Sud, Journal of Materials Research and Technology 8, 3995-4009, (2019); https://doi.org/10.1016/j.jmrt.2019.07.008
[14] X.-K. Wang, C. Wang, W.-Q. Jiang, W.-L. Guo, J.-G. Wang, Chemical Engineering Journal 189-190, 288-294, (2012); https://doi.org/10.1016/j.cej.2012.02.078
[15] Y. Yang, X. Yang, Q. Jia, S. Zheng, Z. Lin, Z. Qin, Vacuum 207, 111577, (2023). https://doi.org/10.1016/j.vacuum.2022.111577
[16] C. D. Valentin, G. Pacchioni, A. Selloni, S. Livraghi, E. Giamello, The journal of physical chemistry B 109, 11414-11419, (2005); https://doi.org/10.1021/jp051756t
[17] K. Batalovic, N. Bundaleski, J. Radakovic, N. Abazovic, M.Mitric, R. A. Silva, M. Savic, J. Belosevic-Cavor, Z. Rakocevic, C.M. Rangel, Physical Chemistry Chemical Physics 19, 7062-7071, (2017); https://doi.org/10.1039/C7CP00188F
[18] P.-P. Filippatos, N. Kelaidis, M. Vasiopoulou, D. Davazoglou, N. N. Lathiotakis, A. Chroneos, Scientific Reports 9, 19970, (2019); https://doi.org/10.1038/s41598-019-55518-8
[19] F. Maleki, G. D. Liberto, G. Pacchioni, ACS Applied Materials & Interfaces 15 (8), 11216-11224, (2023); https://doi.org/10.1021/acsami.2c19273
[20] A. F. Alkai, T. A. Kandiel, F. H. Hussein, R. Dillert, D. W. Bahnemann, Catalysis Science & Technology 3, 3216-3222, (2013); https://doi.org/10.1039/C3CY00494E
[21] M. Padmini, T. Balaganapathi, P. Thilakan, Ceramics International 48 (12), 16685-16694, (2022); https://doi.org/10.1016/j.ceramint.2022.02.217
[22] N. D. Johari, Z. M. Rosli, J. M. Juoi, Journal of Materials Science: Materials in Electronics 33, 15143-15155, (2022); https://doi.org/10.1007/s10854-022-08433-0
[23] J. Krysa, M. Keppert, J. Jirkovsky, V. Stengl, J. Subrt, Materials Chemistry and Physics 86, 333-339, (2004); https://doi.org/10.1016/j.matchemphys.2004.03.021
[24] M. J. Uddin, F. Cesano, A. R. Chowdhury, T. Trad, S. Cravanzola, G. Martra, L. Mino, A. Zecchina, D. Scarano, Frontiers in Materials 7, 192, (2020); https://doi.org/10.3389/fmats.2020.00192
[25] A. K. Chakraborty, S. Ganguli, Md A. Sabur, Journal of Water Process Engineering 55, 104183, (2023); https://doi.org/10.1016/j.jwpe.2023.104183
[26] T. Morikawa, R. Asahi, T. Ohwaki, K. Aoki, Y. Taga, Japanese Journal of Applied Physics 50, L561, (2001); https://doi.org/10.1143/JJAP.40.L561